1-1-2006

Enhanced third-order nonlinear effects in optical AlGaAs nanowires

G. A. Siviloglou
University of Central Florida

S. Suntsov
University of Central Florida

R. El-Ganainy
University of Central Florida

R. Iwanow
University of Central Florida

G. I. Stegeman
University of Central Florida

See next page for additional authors

Enhanced third-order nonlinear effects in optical AlGaAs nanowires

G. A. Siviloglou, S. Suntsov, R. El-Ganainy, R. Iwanow, G. I. Stegeman, and D. N. Christodoulides

College of Optics & Photonics-CREOL & FPCE, University of Central Florida, Orlando, Florida, 32816
george@creol.ucf.edu

R. Morandotti

National Institute of Scientific Research, University of Quebec, Quebec J3X 1S2, Canada

D. Modotto, A. Locatelli, and C. De Angelis

Istituto Nazionale per la Fisica della Materia, Dipartimento di Elettronica per l'Automazione, Università di Brescia,via Branze 38, Brescia 25123, Italy

F. Pozzi, C. R. Stanley, and M. Sorel

Department of Electrical and Electronic Engineering, University of Glasgow, Glasgow G12 8QQ, Scotland
M.Sorel@elec.gla.ac.uk

Abstract: We report the first observation of enhanced third-order nonlinear effects in AlGaAs nanowires. AlGaAs nanowaveguides with widths varying from 100 to 600nm were fabricated and characterized. Nonlinear phase shifts of ~π were experimentally observed at 1.55μm with peak powers of 30-40W in 600μm long, 550nm wide guides.

OCIS codes: (190.0190) Nonlinear optics; (190.3270) Kerr effect; (190.4180) Multiphoton processes; (190.5940) Self-action effects; (160.4330) Nonlinear optical materials.

References and links

1. L. Tong, R. R. Gattass, J. B. Ashcom, S. He, J. Lou, M. Shen, I. Maxwell, and E. Mazur, "Subwavelength-diameter silica wires for low-loss optical wave guiding," Nature **426**, 816-819 (2003).
2. P. N. Prasad, *Nanophotonics*, (John Wiley and Sons, New York, 2004).
3. J. C. Knight, "Photonic crystal fibers," Nature **424**, 847-851 (2003).
4. S. G. Leon-Saval, T. A. Birks, W. J. Wadsworth, P. St. J. Russell, and M. W. Mason, "Supercontinuum generation in submicron fibre waveguides," Opt. Express **12,** 2864-2869 (2004).
5. Y. K. Lizé, E. C. Mägi, V. G. Ta'eed, J. A. Bolger, P. Steinvurzel, and B. J. Eggleton, "Microstructured optical fiber photonic wires with subwavelength core diameter," Opt. Express **12,** 3209-3217 (2004).
6. M. A. Foster, A. L. Gaeta, Q. Cao, and R. Trebino, "Soliton-effect compression of supercontinuum to few-cycle durations in photonic nanowires," Opt. Express **13,** 6848-6855 (2005).
7. H. Ebendorff-Heidepriem, P. Petropoulos, S. Asimakis, V. Finazzi, R. C. Moore, K. Frampton, F. Koizumi, D. J. Richardson, and T. M. Monro, "Bismuth glass holey fibers with high nonlinearity," Opt. Express **12,** 5082-5087 (2004).
8. G. Brambilla, F. Koizumi, V. Finazzi, and D. J. Richardson, "Supercontinuum generation in tapered bismuth silicate fibres," Electron. Lett. **41,** 795-797 (2005).
9. V. V. Ravi Kanth Kumar, A. K. George, J. C. Knight, and P. St. J. Russell, "Tellurite photonic crystal fiber," Opt. Express **11**, 2641-2645 (2003).
10. G. Brambilla, F. Koizumi, X. Feng, and D. J. Richardson, "Compound-glass optical nanowires," Electron. Lett. **41,** 400-402 (2005).
11. L. Tong, L. Hu, J. Zhang, J. Qiu, Q. Yang, J. Lou, Y. Shen, J. He, and Z. Ye, "Photonic nanowires directly drawn from bulk glasses," Opt. Express **14,** 82-87 (2006).

#73069 - $15.00 USD Received 17 July 2006; accepted 27 September 2006

12. A. R. Cowan, G. W. Rieger, and J. F. Young, "Nonlinear transmission of 1.5 μm pulses through single-mode silicon-on-insulator waveguide structures," Opt. Express **12**, 1611-1621 (2004)
13. H. Yamada, M. Shirane, T. Chu, H. Yokoyama, S.Ishida, and Y. Arakawa, "Nonlinear-Optic Silicon-Nanowire Waveguides," Jpn. J. Appl. Phys. **44**, 6541-6545 (2005).
14. E. Dulkeith, Y. A. Vlasov, X. Chen, N. C. Panoiu, and R. M. Osgood, Jr., "Self-phase-modulation in submicron silicon-on-insulator photonic wires," Opt. Express **14**, 5524-5534 (2006)
15. G.I. Stegeman, A. Villeneuve, J.S. Aitchison and C.N. Ironside, "Nonlinear Integrated Optics and All-optical Switching in Semiconductors", book chapter in *Fabrication, Properties and Applications of Low-Dimensional Semiconductors*, edited by M. Balkanski and I. Yanchev, NATO ASI Series (Kluwer Academic Publishers, Dordrecht, 1995), pp. 415-449.
16. G.I. Stegeman, A. Villeneuve, J. Kang, J.S. Aitchison, C.N. Ironside, K. Al-hemyari, C.C. Yang, C-H. Lin, H-H. Lin, G.T. Kennedy, R.S. Grant and W. Sibbett, "AlGaAs Below Half Bandgap: The Silicon of Nonlinear Optical Materials," Int. J. Nonlinear Opt. Phy. **3,** 347-371 (1994).
17. R. El-Ganainy, S. Mokhov, K.G. Makris, D.N. Christodoulides, and R. Morandotti, "Solitons in dispersion-inverted AlGaAs nanowires," Opt. Express **14**, 2277-2282 (2006).
18. L. Scaccabarozzi, X. Yu, M. L. Povinelli, S. Fan, M. M. Fejer and J. S. Harris, "Highly Efficient Birefringent Second Harmonic Generation in Submicron AlGaAs/Al_xO_y Waveguides," CLEO 2005 Technical Digest, paper CPDA10.
19. V. Van, T. A. Ibrahim, P. P. Absil, F. G. Johnson, R. Grover, and P.-T. Ho, "Optical Signal Processing Using Nonlinear Semiconductor Microring Resonators," IEEE Journal of Selected Topics in Quantum Electronics, **8,** 705-713 (2002).
20. J. E. Heebner, N. N. Lepeshkin, A. Schweinsberg, G. W. Wicks, R. W. Boyd, R. Grover, and P.-T. Ho, "Enhanced linear and nonlinear optical phase response of AlGaAs microring resonators," Opt. Lett. **29**, 769-771 (2004).
21. J. U. Kang, A. Villeneuve, M. Sheik-Bahae, G. I. Stegeman, K. Al-hemyari, J. S. Aitchison, and C. N. Ironside, "Limitation due to three-photon absorption on the useful spectral range for nonlinear optics in AlGaAs below half band gap," Appl. Phys. Lett. **65,** 147-149 (1994).
22. R. J. Deri and M. A. Emanuel, "Consistent formula for the refractive index of $Al_xGa_{1-x}As$ below the band edge," J. Appl. Phys. **77**, 4667-4672 (1995).
23. G. P. Agrawal, *Nonlinear Fiber Optics*, (Academic Press, San Diego, 2001).

1. Introduction

The development of single-mode nanowaveguides (or nanowires) is today an issue of great research interest [1]. Advances in fabrication technology over the last decade have made it possible to fabricate devices with sub-micron and nano-scale transverse dimensions. In the future, these sub-wavelength waveguides may find applications as compact information conduits between microchip devices or as sensors in biotechnology [2]. In general, optical nanowaveguide structures are capable of providing superior light confinement (because of their strong index contrast) and are thus ideal for nonlinear optics applications [3]. To date, silica glass waveguides and fibers have been fabricated with sub-micron modal diameters and have been used to observe super-continuum generation and soliton compression among other nonlinear effects [4-6]. In addition, other nonlinear glasses such as lead silicate, tellurites, and bismuth have been employed in similar ways [7-11]. Lately self-phase modulation has also been observed experimentally in silicon nanowires [12-14]

Quite recently we have explored the fabrication of high index-contrast AlGaAs nanowires. Given the fact that at 1.55μm AlGaAs exhibits an ultrafast Kerr nonlinearity that is three orders of magnitude higher than that of silica [15, 16], the prospect of realizing sub-μm^2 cross-section nanowires may eventually lead to low-power nonlinear devices with *sub-millimeter* interaction lengths operating at *Watt power levels* [17]. We note that second harmonic generation in AlGaAs optical nanowaveguides has also been recently demonstrated [18] and nonlinear micro-ring resonators have been realized in this same material system [19, 20].

In this paper we report the first observation of self-phase-modulation enhancement due to strong confinement in 550 nm wide, Kerr nonlinear AlGaAs nanowaveguides. We have successfully fabricated and tested prototype AlGaAs optical nanowires for all-optical applications. The prototype structures fabricated were a few hundred nanometers wide and up

#73069 - $15.00 USD Received 17 July 2006; accepted 27 September 2006

to 700 μm long. To facilitate in-coupling and out-coupling from such narrow waveguides, tapers were also fabricated for efficient excitation and output collection. The propagation losses were evaluated and the spectral broadening or self-phase-modulation (SPM) and nonlinear three photon absorption were measured and compared to that of conventional waveguides of the same length. Large enhancements in SPM compared to standard ridge waveguides were observed. Our experimental results were in excellent agreement with theoretical predictions based on the bulk value for n_2 [15, 16]. Furthermore, the three photon absorption coefficient in these nanowires as determined from nonlinear absorption measurements was also comparable to that in the bulk [21].

2. Nanowaveguide Fabrication

The nanowires were fabricated by deep etching of a multilayer MBE structure on a GaAs wafer. The nanowaveguide structure and the required fabrication steps in the vertical direction are shown in Figure 1.

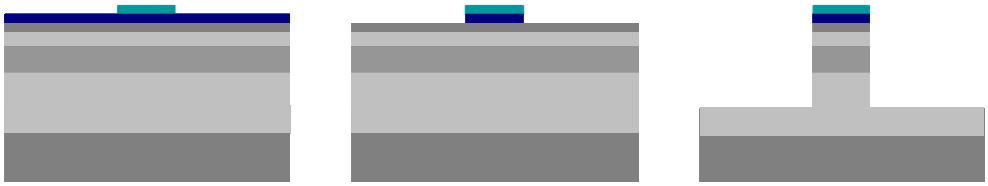

Fig. 1. Schematic of the nanowaveguide fabrication process. The first figure shows the deposited PECVD SiO_2 (blue) onto the AlGaAs multilayer structure, and the definition of waveguides using e-beam lithography and PPMA resist (green). The second one shows the etching of the PECVD SiO_2 mask using C_2F_6. The third one shows the semiconductor rib after deep etching with $SiCl_4$.

The substrate is GaAs on top of which was deposited sequentially a 4200nm cladding layer of $Al_{0.7}Ga_{0.3}As$, a 500 nm core of $Al_{0.2}Ga_{0.8}As$, a 300 nm upper cladding of $Al_{0.7}Ga_{0.3}As$ and a cap layer of 100nm GaAs. The layer structure was etched down to a depth of 2300 nm, (as shown in the SEM picture of Fig. 2), to form a single mode waveguide at 1550 nm.

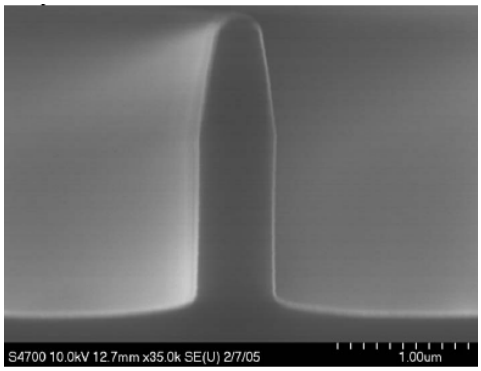

Fig. 2. SEM picture of the nanowire rib waveguide on a GaAs substrate.

The structure of each completed waveguide, as viewed from the top is shown in Fig. 3. The total length of each device was 1.8mm.The length L of the nanowire was varied from 0 to 700μm in 100μm steps to facilitate the measurement of the nanowire losses. Although a large variety of nanowire widths W was successfully fabricated, all of the experiments were performed with W≅550nm guides.

#73069 - $15.00 USD Received 17 July 2006; accepted 27 September 2006

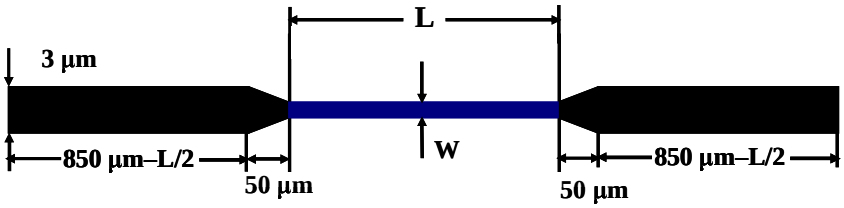

Fig. 3. Single channel as viewed from above (in the plane of the substrate).

In order to analyze the modal vector field structure of such high index contrast waveguides a finite element method was used. Since the aluminum content is known in every layer, the corresponding refractive index can be obtained [22] and the resulting field distributions for the lowest TM and TE modes at 1550 nm can be computed as shown in Fig. 4 below.

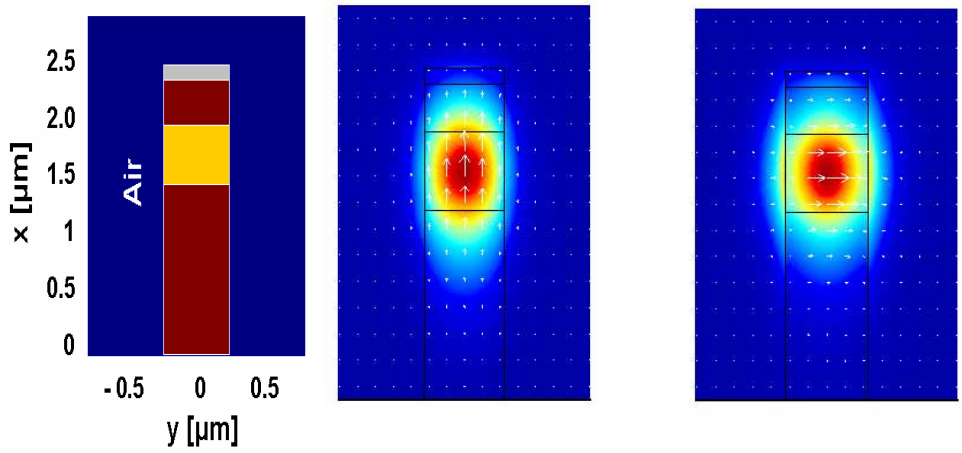

Fig. 4. The refractive index profile of the nanowaveguide used (left). The TM mode field profile (center) is primarily x-polarized whereas the TE mode field distribution (right) is mostly polarized in the y-direction.

As Fig. 4 shows, strong modal confinement is obtained for the TM mode. The modal area of the single mode guide is in this case ~ 0.3 μm^2. This value is approximately two-orders of magnitude lower when compared with typical weakly guiding channel waveguides with modal areas of the order 10-15μm^2 [23].

3. Linear and nonlinear transmission measurements

Rough estimates for the propagation loss for different nanowire lengths were first obtained by measuring the transmission of the devices at low powers as a function of the nanowire length L. Typical results are shown in Fig. 5 for a nanowire of width 550nm. Assuming constant values for the in- and out-coupling efficiencies and the tapered regions, the total measured loss for the fundamental TM mode was found to vary with length L. For the TM polarized mode the average loss value of the nanowire was estimated to be ~19 cm^{-1}. On the other hand, the TE modes exhibited a higher loss in the nanowire section, presumably because in this case the fields are perpendicular to the boundaries (as compared to the TM case, see Fig. 4) and hence are more sensitive to waveguide surface roughness etc.

#73069 - $15.00 USD Received 17 July 2006; accepted 27 September 2006

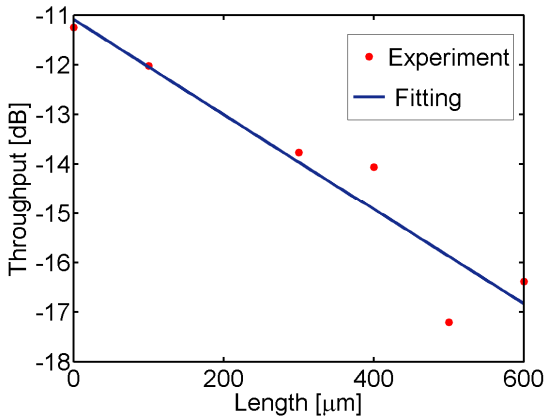

Fig. 5. Device transmission (red dots) as a function of nanowire length for a 550nm wide nanowire was measured as the ratio of the throughput-power just before the output objective lens to the input power just after the input objective lens. The nanowire loss coefficient was estimated form the slope of the blue solid line which takes into account a 29% coupling efficiency and 29% Fresnel losses in the input and output facets.

Although a number of channels of different channel lengths were investigated, here we focus first on the case L=0 to obtain the coupling efficiency and the losses in the input, output waveguide sections. In experiments with a cw laser, the contrast in the Fabry-Perot fringes due to multi-reflections between the sample facets yielded a loss coefficient of $4cm^{-1}$ for the structure. In subsequent calculations, since the short tapers were designed to be adiabatic transformers, i.e. non-radiative, the $4cm^{-1}$ measured loss was attributed to the total length of the structure. Furthermore, using the throughput measurements for L=0 and the Fresnel losses at the two interfaces (29% each), a coupling efficiency due to field overlap of 29% was deduced and used in subsequent calculations.

Since the nanowire effective area is only $0.3\mu m^2$, the intensities easily approach 3 GW/cm^2 with peak powers of just 10W. Hence multi-photon absorption was expected to be significant at high intensities. The apparatus used for measuring the nonlinear transmission (and spectral broadening) is shown in Figure 6 below. The optical source was a Pritel fiber laser that was first temporally broadened by a chirped fiber grating, next amplified by a broad area KEOPSYS erbium-doped amplifier and finally compressed by a grating pair to produce 8ps long pulses at a 5MHz repetition rate. The pulses were approximately transform-limited and the maximum peak power output was 4 KW.

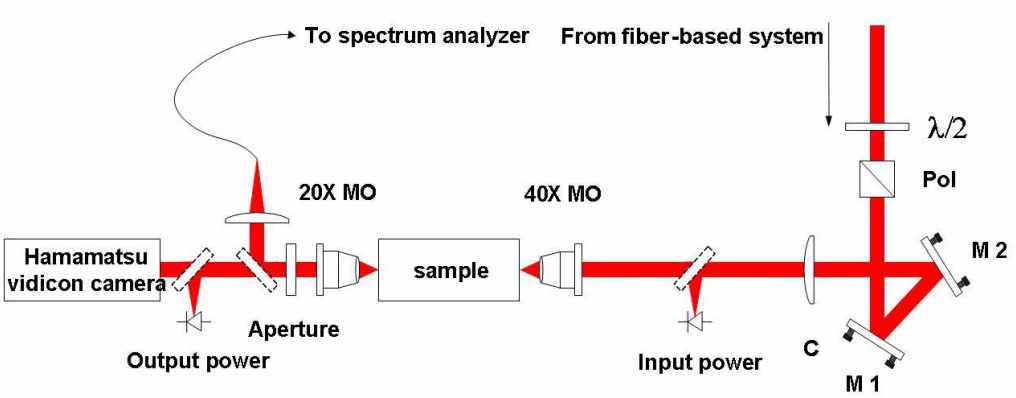

Fig. 6. Apparatus used for measuring the nonlinear transmission and spectral broadening.

#73069 - $15.00 USD
Received 17 July 2006; accepted 27 September 2006

Detailed measurements of the TM throughput between the two sample facets are shown below for 550nm wide nanowire samples with L=0 and L=400μm as a function of the input power just inside the input facet. It is clear from Fig. 7 that at powers of 10W nonlinear absorption is already important. In general, the peak waveguide intensity with propagation distance can be written as

$$\frac{dI}{dz} = -\alpha_1 I - \alpha_2 I^2 - \alpha_3 I^3, \tag{1}$$

where α_1, α_2 and α_3 are the one (linear), two and three photon absorption coefficients respectively. Because the photon energy used is sufficiently less than half the semiconductor's band gap energy, two photon absorption was neglected. The contributions to the transmission loss of the net power $P_{in} = P(0)$ just inside the entrance facet to just inside the exit facet P_{out} were taken into account by the equation:

$$P_{out} = P_{in} - \int_0^{1.8mm} \left[\alpha_1(z)P(z) + \alpha_3 \left(\frac{P(z)}{A_{eff}(z)} \right)^2 P(z) \right] dz \tag{2}$$

where A_{eff} is the effective waveguide cross-section area of each of the three segments of the waveguide: nanowire section and the input and output waveguide sections. The calculated waveguide transmission in Fig. 7 of the L=0 sample (blue line) was based on the measured coupling efficiency, Fresnel losses, the propagation losses just discussed and the literature value for α_3. The linear regime of the throughput curves for the L=400μm nanowire was then used to evaluate the nano-wire loss coefficient and a value of 19cm^{-1} was deduced, in good agreement with the estimates from Fig. 5. Note that the overall agreement between experiment and theory is indeed very good, vindicating the assumption of nonlinear loss via three photon absorption.

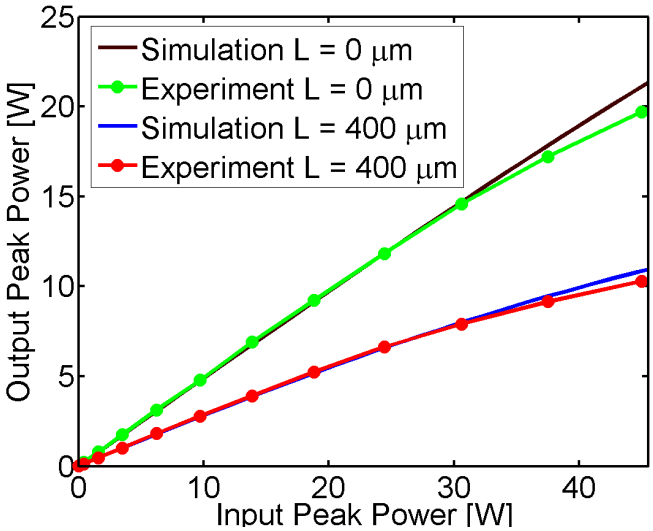

Fig. 7. The throughput of the device versus the power input into the nanowire. The data is shown by the solid circles and the theory using the measured linear loss and the literature value of the three photon absorption coefficient is shown by the solid lines.

#73069 - $15.00 USD Received 17 July 2006; accepted 27 September 2006

4. Self-phase-modulation measurements

A single-mode fiber was used to couple the output from the composite waveguides to the spectrum optical analyzer (SOA). The spectrum obtained at the output is shown in Figure 8 for the L=0 and L=600μm nanowire lengths with W=550nm. (The choice of L=600μm was made to optimize the SPM of the nanowire relative to the input and output sections: The L= 700μm nanowire had a damaged input facet.) Although the combined length of the input and output channels is about 2 times that of the nanowire, the nonlinear phase shift in the nanowire clearly dominates the spectrum.

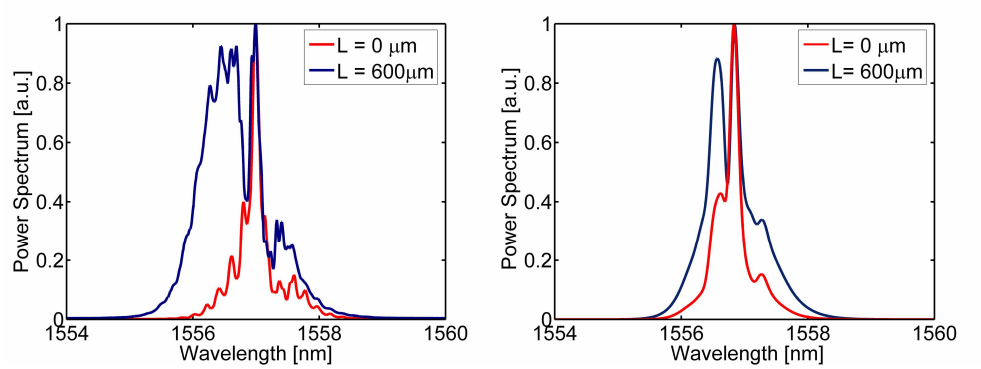

Fig. 8. Spectral broadening measured for the L=0 and 600μm samples for an input power into the input facet of the sample of 38W (left). Simulations of the spectral broadening (right) obtained using the measured pulse temporal profile (retrieved from SHG FROG), the waveguide transmission parameters, and the known value of n_2=1.5x10^{-13} cm^2/W. The nonlinear phase shift deduced by matching simulations to experiment for the nanowire was 0.9π.

The modeling for the frequency spectrum is complicated because there are both linear and higher order absorption mechanisms that must be taken into account when evaluating the nonlinear phase shifts experienced by the propagating field *U(z,T)*. The pertinent equations are:

$$U(z,T) \propto U(0,T)\exp\left(ik_0 n_2 \int_0^z \frac{1}{A_{eff}(z')} \left\{ P_{in}(T) - \int_0^{z'} \left[\alpha_1(z'')P(z'',T) + \alpha_3 \left(\frac{P(z'',T)}{A_{eff}(z'')} \right)^2 P(z'',T) \right] dz'' \right\} dz' \right) \quad (3)$$

$$\tilde{S}(z,\omega) = \left| \int_{-\infty}^{+\infty} U(z,T)\exp(i\omega T)\, dT \right|^2 \quad (4)$$

where *U(0,T)* is the input field and $\tilde{S}(z,\omega)$ is the frequency power spectrum of the output pulse from the waveguide structure. As Fig. 8 indicates, there is very good agreement between the experiment and the simulation for a total peak nonlinear phase shift of 0.9π.

Fig. 9 shows the change in the frequency spectrum measured at the waveguide output for two different input power levels, namely 8W and 38W (calculated after the input facet of the structure). Again the agreement between experiment and simulation is very good.

#73069 - $15.00 USD Received 17 July 2006; accepted 27 September 2006

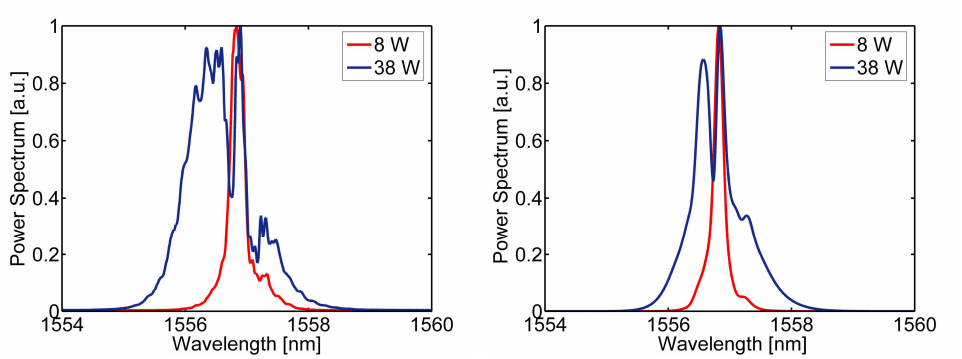

Fig. 9. The power spectrum measured (left-hand-side) and simulated (right-hand-side) for a sample with L=600μm and W=550nm at two different input power levels.

5. Summary

In summary, we have fabricated AlGaAs nanowaveguides with very strong confinement. In spite of high losses, these prototype nanowires were orders of magnitude more efficient in producing a nonlinear phase shift (and hence spectral broadening) than the more conventional waveguides which have been used previously for all-optical devices such as nonlinear directional couplers [15,16]. Such tightly confined waveguides may be used in the future to realize all-optical switching devices operating at greatly reduced (>2 orders of magnitude) power levels that can also be integrated at much higher packing densities.

This research was sponsored in the United States by NSF, in Canada by NSERC, in the UK by EPSRC.

#73069 - $15.00 USD Received 17 July 2006; accepted 27 September 2006